J Neurophysiol 102: 28–40, 2009.
First published April 29, 2009; doi:10.1152/jn.00169.2009.

Dynamic Characterization of Agonist and Antagonist Oculomotoneurons During Conjugate and Disconjugate Eye Movements

Marion R. Van Horn and Kathleen E. Cullen
Aerospace Medical Research Unit, Department of Physiology, McGill University, Montreal, Quebec, Canada

Submitted 25 February 2009; accepted in final form 23 April 2009

Van Horn MR, Cullen KE. Dynamic characterization of agonist and antagonist oculomotoneurons during conjugate and disconjugate eye movements. *J Neurophysiol* 102: 28–40, 2009. First published April 29, 2009; doi:10.1152/jn.00169.2009. In this report, we provide the first quantitative characterization of the relationship between the spike train dynamics of medial rectus oculomotoneurons (OMNs) and eye movements during conjugate and disconjugate saccades. We show that a simple, first-order model (i.e., containing eye position and velocity terms) provided an adequate model of neural discharges during both ON and OFF-directed conjugate saccades, while a second-order model, which included a decaying slide term, significantly improved the ability to fit neuronal responses by ~10% ($P < 0.05$). To understand how the same neurons drove disconjugate eye movements, we evaluated whether sensitivities estimated during conjugate saccades could be used to predict responses during disconjugate saccades. For the majority of neurons (68%), a conjugate-based model failed, and instead neurons preferentially encoded the position and velocity of the ipsilateral eye. Similar to our previous results with abducens motoneurons, we also found that position and velocity sensitivities of OMNs decreased with increasing velocity, and the simulated population drive of OMNs during disconjugate saccades was less (~10%) than during conjugate saccades. Taken together, our results provide evidence that the activation of the antagonist, as well as agonist, motoneuron pools must be considered to understand the neural control of horizontal eye movements across different oculomotor behaviors. Moreover, we propose that the undersampling of smaller motoneurons (e.g., nontwitch) was likely to account for the missing drive observed during disconjugate saccades; these cells are thought to be more specialized for vergence movements and thus could provide the additional input required to command disconjugate eye movements.

INTRODUCTION

To precisely accomplish a desired eye movement, the appropriate neural command must be sent to the extraocular muscles. During saccades, extraocular motoneurons generate a burst of activity (i.e., pulse) that compensates for the resistance of the muscles and orbital tissues. Then at the end of the saccade, motoneurons generate a higher tonic discharge (i.e., step) to resist against the natural elastic recoil of the orbital tissues and hold the eye at a new desired position. Robinson (1964) proposed that the relationship between motoneuron activity and muscle force could be approximated using a fourth-order linear model. Subsequent analysis of the "pulse-step" nature of medial and lateral rectus motoneurons led to the prediction that a first-order model, including the neuron's discharge when the eye is in the center of the orbit, as well eye velocity and position sensitivities, could provide a simpler yet useful model for approximating the firing rate of extraocular motoneurons during conjugate saccades (Robinson 1970; Robinson and Keller 1972).

To verify the original predictions made by Robinson and colleagues, a detailed analysis of abducens motoneurons (ABNs) has since been conducted. Van Gisbergen and colleagues (1981) proposed that including an accelerating term would provide a better description of ABN discharges during saccades. However, a major limitation of the analysis used in this study was that the relative contribution of terms could not be objectively determined. More recently, Sylvestre and Cullen (1999) evaluated the importance of each term by directly fitting the neuronal responses of ABNs during saccades. They found that the addition of both an acceleration term and a slide term, which is used to explain the exponential decay of neuron's firing rate, notably improved their ability to describe the discharge dynamics during saccades. Overall, however, they concluded that a first-order linear model provided an adequate description of the discharge dynamics of ABNs during saccades, smooth pursuit, and vestibular nystagmus. Sylvestre and Cullen (2002) further demonstrated that this same model could be used to describe the discharge dynamics of ABNs during disconjugate saccades (i.e., saccades with changes in viewing distance and eccentricity). Notably, this model needed to be expanded to include the movement of each eye (i.e., ipsi- and contralateral). They found the majority of ABNs preferentially encoded the position and velocity of the ipsilateral eye and that the remaining neurons encoded the motion of both eyes to various degrees (Sylvestre and Cullen 2002).

First-order models have proven valuable for describing how extraocular motoneurons control eye movements. However, an assumption that has been made in previous studies is that the agonist drive, sent to the contracting muscle, dictates the dynamics of the movement. In reality, it is the ratio of agonist and antagonist motoneurons activity that positions the eye. Previous studies, which have compared the discharge rates of motoneurons during fixation at different depths, have revealed that for a given position of the eye in the orbit, the majority of ABNs fire at higher rates during convergence than when gaze is relaxed (Gamlin et al. 1989; Mays and Porter 1984). Furthermore, eye velocity and position sensitivities have been found to invariably decrease as a function of the generated eye velocity (Fuchs et al. 1988; Sylvestre and Cullen 1999). For example, slower movements (e.g., pursuit) were found to have higher sensitivities than faster movements (e.g., saccades) (Sylvestre and Cullen 1999). Interestingly, these potentially surprising relationships can be explained if the activity of the antagonist muscle were considered. For example, during slow movements (e.g., pursuit), the majority of antagonist motoneu-

Address for reprint requests and other correspondence: K. E. Cullen, McIntyre Medical Research Bldg., Rm. 1218, 3655, Prom. Sir William Osler, Montreal, PQ, Canada, H3G 1Y6 (E-mail: kathleen.cullen@mcgill.ca).

rons continue to discharge (Sylvestre and Cullen 1999) and hence the contribution of the antagonist muscle could be providing an additional active force that opposes the agonist muscle.

To create a realistic model of eye movements, it is thus necessary to consider the contribution of the antagonist muscle when evaluating motoneuron activity across multiple oculomotor behaviors. However to date, studies have only provided a complete description of the discharge dynamics of lateral rectus motoneurons (i.e., ABNs) in their ON direction. Here we provide the first detailed characterization of the dynamics of individual medial rectus neurons in the oculomotor nucleus (OMNs) during conjugate and disconjugate saccades. To fully assess the drive to the medial rectus muscle, the activity of OMNs is characterized when the medial rectus is contracting and relaxing (i.e., ON and OFF directions). During conjugate saccades, we fit the dynamic discharge of individual OMNs using an approach previously used to describe ABNs and saccadic burst neurons (Cullen and Guitton 1997; Sylvestre and Cullen 1999, 2002). We then determine whether we could use the parameters estimated during conjugate saccades to predict the activity of OMNs during disconjugate saccades. Finally, we compare the responses of OMN to ABNs to get a better understanding of how the agonist and antagonist muscles are working together to ensure accurate three-dimensional viewing.

METHODS

Recordings were made in two rhesus monkeys (*Macaca mulatta*). The monkeys were prepared for chronic extracellular recording using the aseptic surgical procedures described previously (Sylvestre and Cullen 1999). In brief, a stainless steel post was attached to the animal's skull with stainless steel screws and dental acrylic permitting complete immobilization of the animal's head. Two stainless steel recording chambers, oriented stereotaxically toward the oculomotor nucleus on the right and left side of the brain stem, were also secured to the implant. To record binocular eye position, an eye coil (3 loops of Teflon coated stainless steel wire, 18–20 mm diam) was implanted in each eye (Judge et al. 1980). All procedures were approved by the McGill University Animal Care Committee and complied with the guidelines of the Canadian Council on Animal Care.

Behavioral paradigms

During the experiments, monkeys were head-fixed and seated in a primate chair in the dark. Monkeys were trained to follow a red HeNe laser target projected onto a cylindrical screen located 55 cm away from the monkey's eyes (isovergent, ≈3.5° convergence) and red light-emitting diodes (LEDs), with intensities comparable to that of the laser target, positioned between the screen and the monkey. The timing and location of target illumination, data-acquisition and on-line data displays were controlled using REX, a UNIX-based real-time acquisition system (Hayes et al. 1982).

Neuronal responses were recorded during horizontal conjugate and disconjugate saccades and fixation. Ipsilaterally and contralaterally directed conjugate saccades were elicited by stepping the laser target between horizontal positions (±2.5–30°), in 5° increments, in predictable and unpredictable sequences. A horizontal array of 16 LEDs, which were positioned between the screen and the monkey, were used in combination with the laser target to elicit horizontal disconjugate saccades (Sylvestre and Cullen 2002; Sylvestre et al. 2003; Van Horn et al. 2008; Waitzman et al. 2008). In particular, an illuminated target changed from one of four mid-sagittal LEDs to an eccentric (i.e., right or left of the midsagittal plane) laser target. During this paradigm, monkeys made saccades with horizontal components of 5–30° in amplitude in both directions, and vergence components with amplitudes of ~4–13°. To elicit disconjugate saccades, in which the movement of the right eye or left eye movement was minimized, four LEDs were aligned with the left eye or right eye at an angle of 45° to the left or right of the mid-sagittal plane. To increase the variety of disconjugate saccades in our data set, trials where the LEDs and laser targets were randomly presented were also included.

Data-acquisition procedures

During the experiments the monkeys sat in a primate chair in the center of a 1-m^3, magnetic eye coil system (CNC Engineering). Horizontal and vertical eye position signals were measured using the magnetic search coil technique (Fuchs and Robinson 1966; Judge et al. 1980). Each eye coil signal was calibrated independently by having the monkey fixate, with one eye masked, a variety of targets at different horizontal and vertical eccentricities and different depths. Position signals were low-pass filtered at 250 Hz (analog 8 pole Bessel filter) and sampled at 1 kHz. Because ocular saccades include very little power >50 Hz (Cullen et al. 1996; Van Opstal et al. 1985; Zuber et al. 1968) eye-position signals were further digitally filtered (with a 51st-order finite-impulse-response filter with a Hamming window and a cut-off at 125 Hz), before being differentiated to obtain eye velocity signals (using 0-phase forward and reverse digital filtering to prevent phase distortion).

Extracellular single-unit activity was recorded using enamel-insulated tungsten microelectrodes [2–10 MΩ impedance, Frederick Haer; for details, see (Sylvestre and Cullen 1999)]. Neurons in the oculomotonucleus were identified on-line based on their stereotypical discharge properties during eye movements (Robinson 1970). The existence of reciprocal connections between oculomotor internuclear neurons (OINs) to the abducens has been well described (Carpenter et al. 1963; Highstein and Baker 1978; Highstein et al. 1982; Maciewicz et al. 1975; Steiger and Buttner-Ennever 1978; Ugolini et al. 2006). In a previous study, in which OINs were identified using antidromic identification and collision testing, <5% of the neurons were identified as OINs (Clendaniel and Mays 1994). Accordingly, the majority of the neurons recorded in this study were most likely motoneurons.

When a neuron was properly isolated, unit activity, horizontal and vertical positions of the right and left eyes, and target position were recorded on a digital audio tape (DAT). The isolation of each neuron was reassessed, off-line during playback. An oculomotoneuron was considered to be adequately isolated only when individual action potential waveforms could be discriminated using a windowing circuit (BAK) during saccades (e.g., see Fig. 1 in Sylvestre and Cullen 1999) and during fixation. Subsequent analysis was performed using custom algorithms (Matlab, The MathWorks).

Data analysis

The eyes are referred to as either ipsi- or contralateral based on their location relative to the recording site. Positive and negative values indicate eye positions that are to the right and left of the central position (i.e., straight ahead), respectively. The movement of the eyes is also reported in terms of conjugate [conjugate = (left eye + right eye)/2] and vergence [vergence = left eye – right eye] coordinates (where the left eye and right eye inputs could be either position or velocity signals). Note vergence velocity signals are positive during convergence and negative during divergence.

The onset and offset of all saccades was determined using a 20°/s saccade velocity criterion. Saccades were categorized as conjugate if the change in vergence angle was <2.5°. Disconjugate saccades during which both eyes moved either ipsi- or contralateral to the recording site and for which one eye moved at least twice as much as

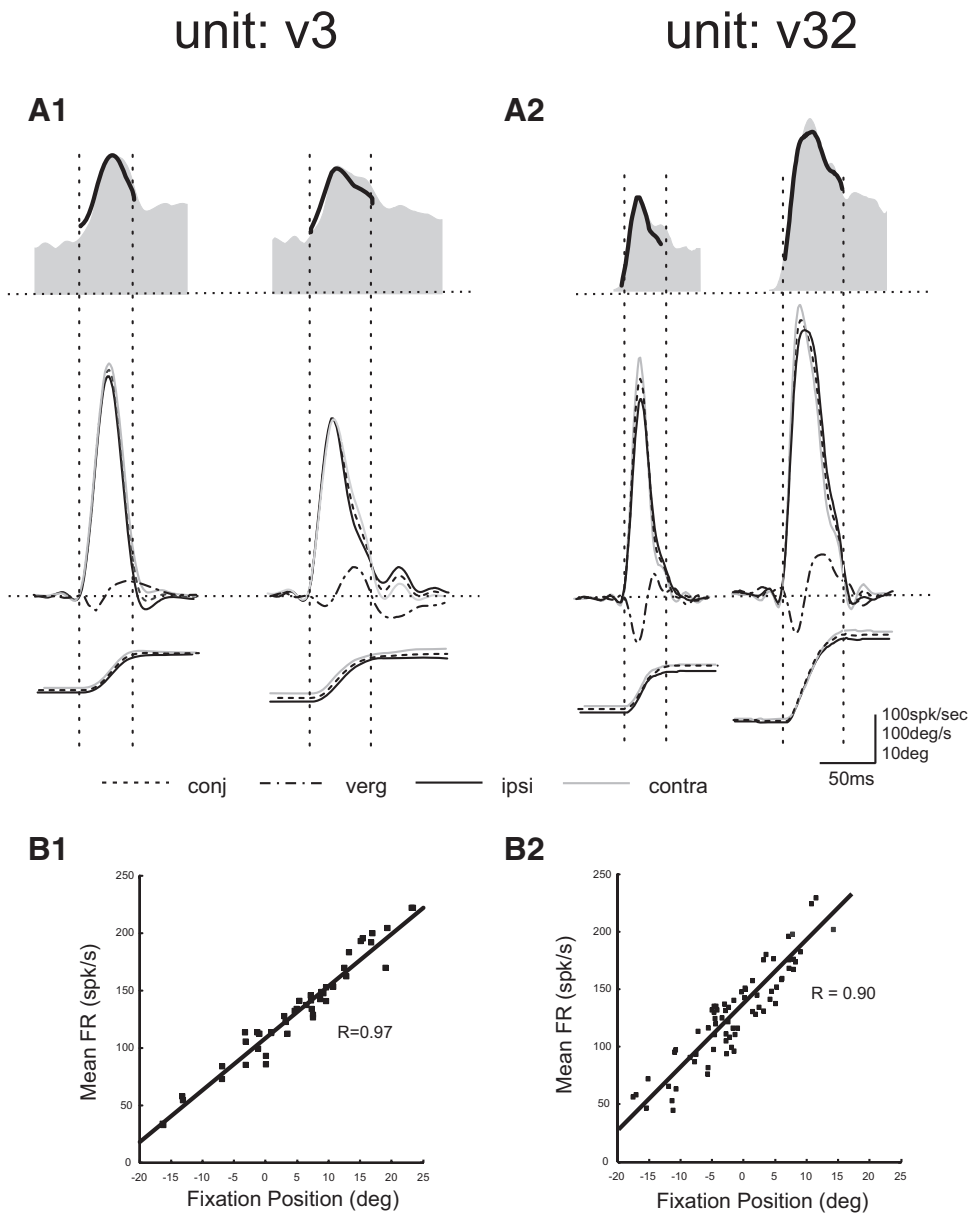

FIG. 1. *A*: discharge patterns of 2 typical oculomotor neurons. Two contralateral (i.e., ON direction) conjugate saccades are shown for each neuron (*1* and *2*). Gray shaded area in the *top row* represents the neurons' firing rate. Superimposed on the firing rate in black is the estimated model fit obtained using a 1st-order model, which included the neuron's discharge when the eye is in the center of the orbit as well eye velocity and position sensitivities. Below the firing rate are the ipsilateral (ipsi), contralateral (contra), conjugate (conj), and vergence (verg) velocities and positions. Note that during conjugate saccades the ipsi- and contralateral eyes move the same amount and have the same dynamics. Horizontal dotted lines represent zero velocity and zero firing rate. Vertical dotted lines denote saccade onset and offset (20°/s); saccade onset and offset (20°/s criterion). *B, 1* and *2*) Mean neuronal firing rate is plotted as a function of mean eye position during fixation for the same 2 neurons shown in *A*.

the other were included in the analysis. Notably, an equal number of converging and diverging saccades were included in the disconjugate dataset to prevent biasing the parameter estimates. Also because previous studies have found that eye velocity and position coefficients are larger during slow velocity movements (Sylvestre and Cullen 1999), the movements included in the conjugate and disconjugate datasets were in the same range of velocity.

For a subset of neurons ($n = 10$), velocity and position sensitivities were estimated and compared across saccades with different velocities. For this analysis, microsaccades and saccades with slow velocity dynamics were included. Microsaccades were defined as short movements with velocities <150°/s, slow saccades were defined eye movements with velocities ranging from 150 to 300°/s and fast saccades were defined as eye movements with velocities ranging from >300°/s.

The linear optimization techniques used to quantify the dynamic sensitivity of a neuron to eye movements, during conjugate saccades (Cullen and Guitton 1996, 1997; Sylvestre and Cullen 1999) and disconjugate saccades (Sylvestre et al. 2002, 2003), have been described previously. The specific linear regression models used in the present study are described in RESULTS. The goodness-of-fit of a given model to the data were quantified using the variance-accounted-for {VAF = 1 − [var (*mod* − *fr*)/var (*fr*)]}, where *mod* represents the modeled firing rate and *fr* represents the actual firing rate. When estimating linear models, the VAF is mathematically equivalent to the correlation coefficient R^2. A VAF value of 1 indicates a perfect fit to the data, and a value of 0 indicates a fit that is equivalent to a mean value. Note that the VAF can be used for the direct comparison of the goodness-of-fit of model estimations and predictions. The dynamic lead time of individual neurons (t_d) was determined during conjugate saccades as described in Sylvestre and Cullen (1999).

For each model parameter in the analysis of disconjugate saccades, we computed 95% confidence intervals using a nonparametric bootstrap approach (Carpenter and Bithell 2000). This analysis method has been described in detail previously and is particularly well suited for small samples with unknown probability distributions (Carpenter and Bithell 2000; Sylvestre and Cullen 2002; Sylvestre et al. 2003; Van Horn and Cullen 2008; Van Horn et al. 2008) and can be used to identify nonsignificant or identical model parameters. Briefly, model parameters in a binocular model (see RESULTS) were estimated from an

original dataset of N (usually >40) disconjugate saccades. Notably, $N/2$ saccades were divergent and $N/2$ saccades were convergent. 1,999 "new data sets" of N saccades were obtained by randomly re-sampling with replacement from the original data set. Therefore every new data set differed from the original data set. After obtaining the new data sets, parameters values were computed for the 1,999 iterations, and the 95% confidence intervals were obtained for each model parameter. Parameter values with 95% confidence intervals that overlapped with zero were nonsignificant and removed from the model Parameters values that overlapped with each other were statistically identical and were replaced with one conjugate parameter. The reduced models were then re-run.

Because adding extra terms to a model invariably improves its goodness of fit, we also calculated the Bayesian information criterion (BIC). The BIC, which served as a "cost index," was calculated for each model estimation to quantitatively determine whether removing the term was justified. If the change in BIC was very small (<0.05), this indicated that the new model described the data as well as the more complex model thereby justifying the removal of the term.

Quantification of ocular preference

Quantification of ocular preference has been described previously (Sylvestre and Cullen 2002; Sylvestre et al. 2003; Van Horn et al. 2008). Briefly, for any given neuron, the sensitivity to the position and velocity of each eye was used to compute a ratio index: Ratio = (smaller estimated parameter value)/(larger estimated parameter value) to indicate which eye provided the larger parameter value (i.e., the neuron's "preferred eye"), each ratio index was assigned an "i" or a "c," for the ipsi- or contralateral eye, respectively. Using the ratio indexes, neurons were assigned to one of five categories, namely; monocular ipsilateral, monocular contralateral, binocular ipsilateral, binocular contralateral or conjugate (see Table 1 in Van Horn et al. 2008 for specific criteria for each category).

Mean values in the text are described as means ± SD. A Student's t-test was used to determine whether the average of two measured parameters differed significantly from each other.

RESULTS

Our analysis approach was the following: first, we characterized the dynamic responses of medial rectus neurons in the OMNs during contralateral (ON direction)- and ipsilateral (OFF direction)-directed conjugate saccades. Second, we assessed whether we could predict the dynamic discharge of OMNs during disconjugate saccades based on their estimated responses during conjugate saccades. Third, we estimated the sensitivity of individual neurons to the velocity and position of the ipsi- and contralateral eye. We then examined the firing rates of individual OMNs across different oculomotor behaviors. In particular, we determined whether the parameters estimated during conjugate saccades could be used to predict the activity of OMNs during fixation, microsaccades, and slower saccades. Moreover, to get a better understanding of how the agonist and antagonist muscles work together, we compared the responses of OMN to abducens motoneurons (ABNs).

TABLE 1. *Average VAFs across population of neurons using conjugate model during conjugate versus disconjugate saccades*

Ocular Category	n	$VAF_{Est\text{-}Conj}$	$VAF_{Pred\text{-}Conj}$	$VAF_{Pred\text{-}Pref\ eye}$
Monocular Ipsilateral	13	0.6 ± 0.09	0.39 ± 0.19	0.50 ± 0.13
Monocular Contralateral	4	0.6 ± 0.09	0.46 ± 0.28	0.55 ± 0.15
Binocular Ipsilateral	2	0.55 ± 0.04	0.1 ± 0.00	0.47 ± 0.24
Binocular Contralateral	2	0.48 ± 0.08	0.63 ± 0.12	0.63 ± 0.23
Conjugate	1	0.45 ± 0.0	0.37 ± 0.00	0.37 ± 0.00
Mean population	22	0.53 ± 0.06	0.39 ± 0.118	0.50 ± 0.22

Data are presented as means ± SD. n, number of units in each category; VAF, variance accounted for; $VAF_{Est\text{-}Conj}$, the VAF when estimating the firing rate during conjugate saccades using the conjugate velocity; $VAF_{Pred\text{-}Conj}$, the VAF when predicting the firing rate during disconjugate saccades using the conjugate velocity; $VAF_{Pred\text{-}Pref\ eye}$, the VAF when predicting the firing rate during disconjugate saccades using the preferred eye velocity.

Dynamic analysis during conjugate saccades

A total of 34 isolated OMNs were analyzed during conjugate saccades. As has been described previously, all neurons increased their firing rates during contralateral (i.e., ON direction) saccades (Gamlin and Mays 1992; Keller 1973; Robinson 1970; Schiller 1970). Figure 1*A, 1* and *2,* illustrates two typical example OMNs during contralateral saccades. We first estimated a neuron's sensitivity to eye movements during ON-directed conjugate saccades using the following dynamic model, which has previously been shown to adequately describe the neuronal discharge of ABNs during conjugate saccades (Sylvestre and Cullen 1999, 2002)

$$FR(t) = b_{CJ} + k_{CJ}\,CJ(t - t_d) + r_{CJ}\,\dot{C}J(t - t_d)$$

where $FR(t)$ is the neuron's instantaneous firing rate, b_{CJ} and k_{CJ} and r_{CJ} are constants that represent the bias and the neuron's horizontal eye position and eye velocity sensitivity estimated during conjugate saccades, respectively. t_d refers to the dynamic lead time and $CJ(t)$ and $\dot{C}J(t)$ refer to the instantaneous horizontal conjugate eye position and velocity, respectively. Model fits are superimposed on the firing rates for the two example neurons shown in Fig. 1*A, 1* and *2.* Similar to ABNs, this first-order model provided a very good fit of OMNs' firing rate [mean population VAF = 0.60 ± 0.1, bias = 116.5 ± 60.346 spike/s, k = 4.44 ± 2.4 (spike/s)/°, r = 0.55 ± 0.32 (spike/s)/(°/s), t_d = 10.4 ± 2.5 ms]. Notably, the addition of an acceleration term did not significantly improve our ability to estimate the neuron's firing rate (mean population VAF = 0.60 ± 0.11, P = 0.46; ΔBIC <0.05), while the addition of both an acceleration term and a slide term [proportional to the derivative of the neuron's firing rate ($c\dot{M}N$)] significantly increased the fit by ~10% (VAF = 0.70 ± 0.09; P < 0.05; c_{OMN} = 23 ± 18 ms). Note the parameter estimates in the present study were similar to those calculated previously for ABNs (c_{ABN} = 15 ± 16 ms) (Sylvestre and Cullen 1999).

Previous studies have shown that the mean firing rate of an OMN is related to eye position during steady periods of fixation (Gamlin and Mays 1992; Keller 1973; Robinson 1970; Robinson and Keller 1972; Schiller 1970). We verified this relationship in our sample of OMNs. During fixation, mean firing rate was correlated to eye position (mean y intercept = 80 ± 97 spike/s, mean slope = 6.3 ± 4.8 (spike/s)/°, mean R^2 = 0.66 ± 0.22). Figure 1*B, 1* and *2,* shows the results of this fixation analysis for the two example neurons. As will be discussed in more detail in the following text, the mean position sensitivity estimated during fixation was significantly larger than that estimated during conjugate saccades {6.4 ± 4.9 vs. 4.4 ± 2.4 [(spike/s)/°]; P < 0.05}.

Dynamic responses estimated during OFF-directed conjugate saccades

To fully assess the drive to the extraocular muscles, the activity of OMNs was also characterized during OFF-directed (i.e., ipsilateral) conjugate saccades. Notably, similar to ABNs, the majority of the neurons (75%) were driven into inhibitory cut-off for very large saccades (>15°) in the OFF direction. We estimated the neuron's sensitivity using the same dynamic model used during conjugate saccades for movements that were not driven into inhibitory cut-off. This first-order model also provided a very good fit of OMNs' firing rate during the OFF direction [mean population VAF = 0.54 ± 0.13, bias = 97.88 ± 36.3 spike/s, k = 4.8 ± 2.7 (spike/s)/°, r = 0.16 ± 0.09 (spike/s)/(°/s]. Model fits estimated during OFF-directed conjugate saccades for the two example neurons shown in Fig. 1 are illustrated for in Fig. 2*A, 1* and *2*.

Example OMN with a preference for the ipsilateral eye

We next determined if the conjugate parameters estimated during conjugate saccades could predict the neuron's activity during disconjugate saccades. Sufficient disconjugate behavior was recorded in 22 of the 34 neurons. Figure 3 shows the activity of the example OMN shown in Figs. 1 and 2 (unit v3) during converging (*A*) and diverging (*B*) disconjugate saccades. Note the large differences in dynamics for the two eyes during these movements: in the converging case (*A*), the ipsilateral eye moved while the contralateral eye was relatively stationary, whereas in the diverging case (*B*), the contralateral eye moved while the ipsilateral eye was relatively stationary. Notably, although the conjugate component of the movements was comparable in the two behaviors, the corresponding firing rates were strikingly different.

Interestingly, for this example neuron, as well as the majority of SBNs (68%) in our study, a conjugate-based prediction tended to undershoot the firing rate when the ipsilateral eye moved more (i.e., during the converging movements for this example neuron, *A*) and to overshoot when the ipsilateral eye moved less (*B*). In fact, the neural activity was best predicted when ipsilateral (Fig. 3; superimposed blue trace; $VAF_{pred\text{-}ipsi} = 0.42$), rather than conjugate or contralateral eye positions and velocities (superimposed black and red traces; $VAF_{pred\text{-}conj} = 0.37$ and $VAF_{pred\text{-}contra} = 0.24$), were the model inputs. The mean VAFs for the population of neurons are presented in Table 1.

The results of the prediction-based analysis suggest that the majority of the OMNs preferentially encode the movement of an individual eye. We next investigated whether a binocular expansion of the conjugate model might provide an improved description of neuronal discharges during disconjugate saccades

$$FR(t) = b + k_i\,IE(t - t_d) + k_c\,CE(t - t_d) + r_i\,\dot{I}E(t - t_d) + r_c\,\dot{C}E(t - t_d)$$

where b, k_i, k_c, r_i, and r_c are the bias, ipsi- and contralateral eye position and velocity sensitivities of the neuron, respectively (subscripts i and c refer to the ipsilateral and contralateral eyes relative to the recording site, respectively), and IE(t), CE(t), $\dot{I}E(t)$, and $\dot{C}E(t)$ are instantaneous ipsi- and contralateral position and eye velocities, respectively. When the parameters of binocular expansion model were freely estimated, a very good

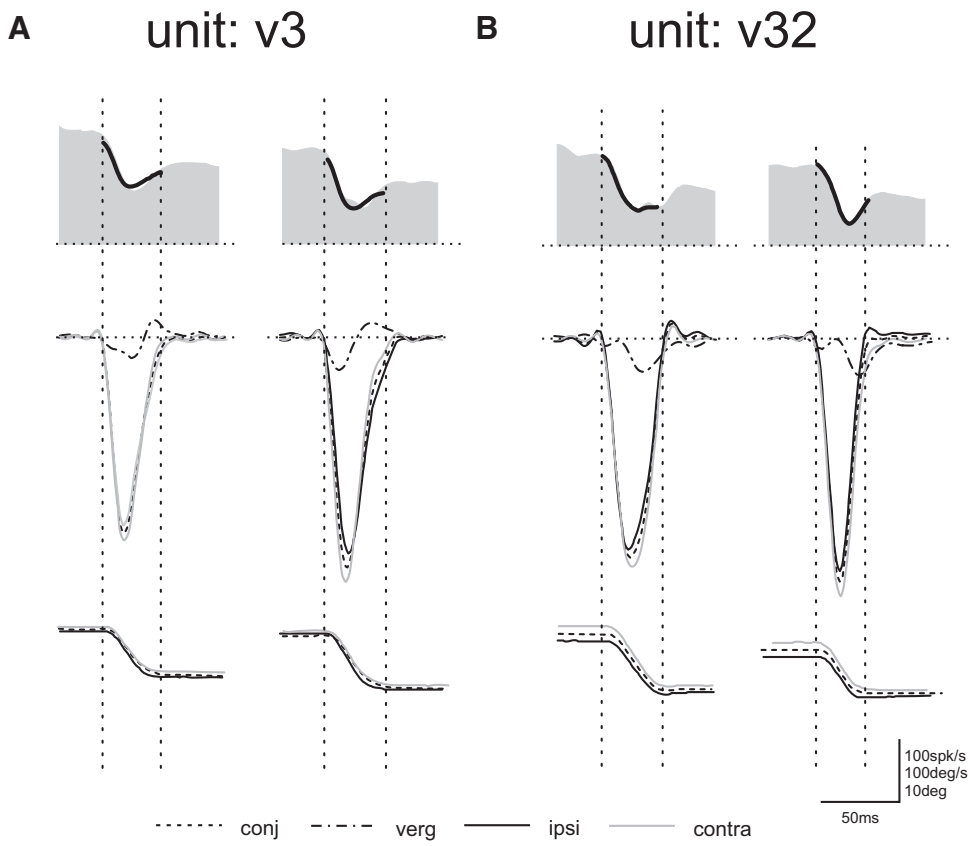

FIG. 2. *A* and *B*: discharge patterns of the same 2 neurons shown in Fig. 1. Two ipsilateral (i.e., OFF direction) conjugate saccades are shown for each neuron. Model fits using a 1st-order model, which included the neuron's discharge when the eye is in the center of the orbit as well eye-velocity and -position sensitivities, are superimposed on the firing rate.

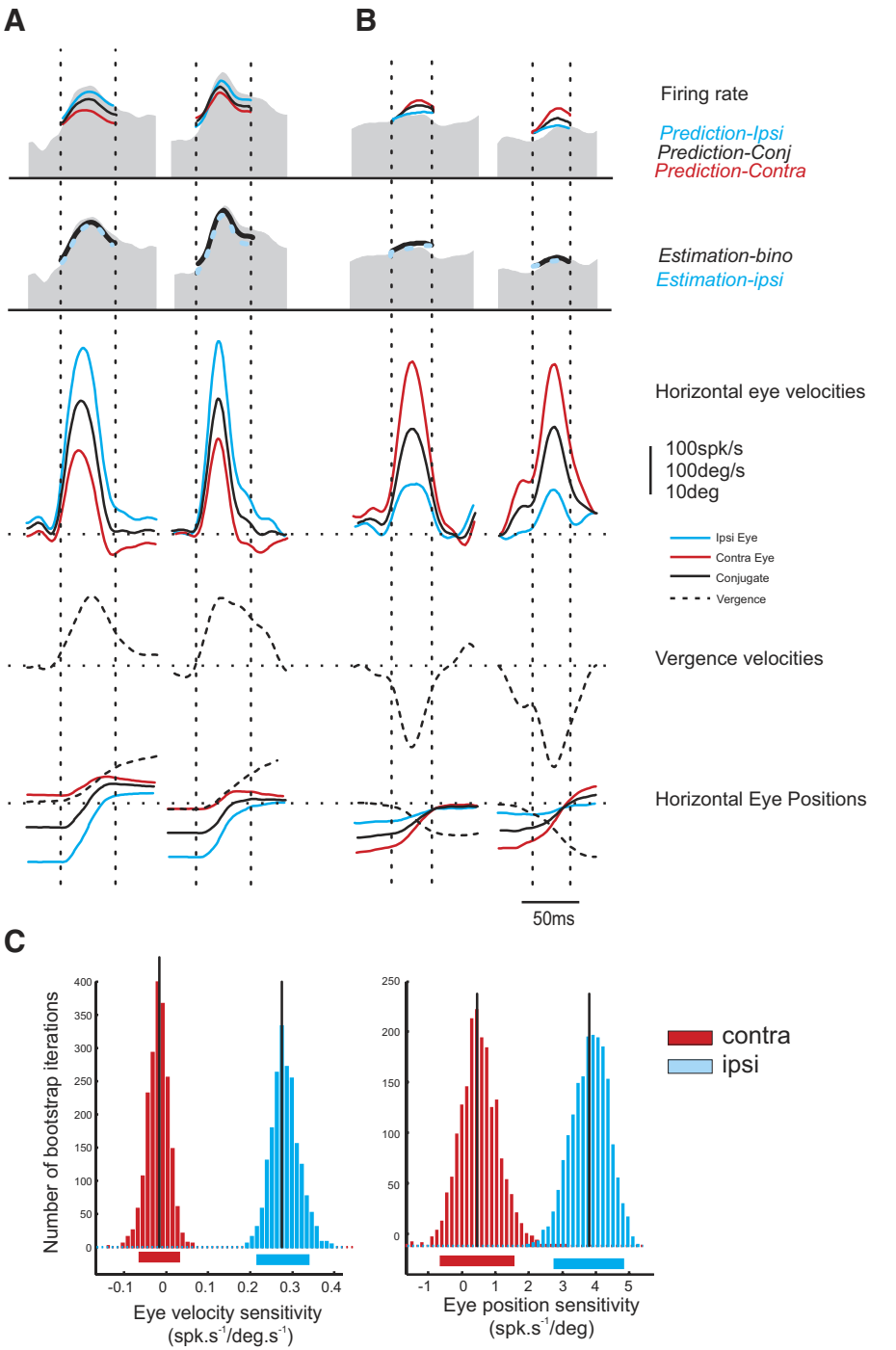

FIG. 3. Discharge patterns of an example monocular neuron during converging (*A*) and diverging (*B*) disconjugate saccades in the neuron's ON direction. The firing rate of the neuron is shown as the gray shaded area (*top row* and reproduced in *2nd row* for clarity). Predicted model fits using ipsilateral, conjugate, and contralateral eye velocities are shown in the *top row* in blue, black, and red, respectively [ipsilateral variance accounted for (VAF_{ipsi} = 0.42, VAF_{conj} = 0.37, VAF_{contra} = 0.24)]. Estimated model fits using the binocular model (black trace) and reduced ipsilateral model (dashed blue trace) are shown in the *2nd row*. Note, VAFs indicated here were calculated when fitting the entire data set. Conjugate, vergence, and vertical velocities and positions (*bottom rows*) are also shown. Dotted vertical lines represent vertical saccade onsets and offsets. *C*: results of bootstrap analysis. *Left*: results for eye velocity sensitivity for this neuron. *Right*: results of eye position sensitivity of this neuron. Histograms represent the distribution of parameter values obtained with the bootstrapping analysis using the binocular model for the contralateral (red) and ipsilateral (blue) eye. Black vertical lines indicate the mean value for each parameter and the thick horizontal bars below the histograms indicate the 95% confidence intervals associated with each parameter. Note the 95% confidence interval for the contralateral eye (red bar) overlaps with zero and is therefore not significantly different from 0.

description of the example OMN's discharge patterns was obtained (Fig. 3, $VAF_{est\text{-}bino}$ = 0.47, *2nd row,* thick black curve).

To determine if all parameters of the binocular expansion model were required to accurately describe the neuron's firing rate, 95% bootstrap confidence intervals were used to reduce the model to its simplest form (see METHODS). The 95% bootstrap confidence intervals revealed that only the ipsilateral eye position (k_i) and ipsilateral velocity-sensitivity term (r_i) and bias were significantly different from zero (Fig. 3C). Removing the contralateral eye position (k_c) and contralateral eye velocity-sensitivity term (r_c) had a negligible impact on our ability to fit this neuron's discharge (blue dashed curve, *2nd row,* Fig. 3; $VAF_{est\text{-}ipsi}$ = 0.46, $\Delta BIC < 0.05$). We therefore conclude that this neuron is monocular with a preference for the ipsilateral eye. The average estimated VAFs and differences in BIC (i.e., ΔBIC) provided by the complete binocular versus reduced models for all neurons is summarized in Table 2.

Response of OFF-directed disconjugate saccades

To fully assess the drive to the extraocular muscles, the activity of OMNs was also characterized during OFF-directed disconjugate saccades. Fig. 4 shows the activity of the same

TABLE 2. *Average VAFs and ΔBICs across population of neurons during disconjugate saccades using binocular versus reduced models*

Ocular Category	*n*	$VAF_{Est\text{-}Bino}$	$VAF_{Est\text{-}Reduced}$	ΔBIC
Monocular Ipsilateral	13	0.57 ± 0.15	0.56 ± 0.14	<0.05
Monocular Contralateral	4	0.61 ± 0.16	0.60 ± 0.16	<0.05
Binocular Ipsilateral	2	0.32 ± 0.09	0.32 ± 0.09	<0.05
Binocular Contralateral	2	0.79 ± 0.06	0.79 ± 0.06	<0.05
Conjugate	1	0.40 ± 0.00	0.40 ± 0.05	<0.05
Mean population	22	0.54 ± 0.09	0.53 ± 0.1	<0.05

Abbreviations: *n,* number of units; VAF, variance-accounted-for: BIC, Bayesian information criteria. $VAF_{Est\text{-}bino}$, the VAF when estimating using both eyes as model inputs; $VAF_{Est\text{-}Reduced}$, the VAF when estimating using the reduced model with the preferred eye as the model input. i.e., conjugate, ipsilateral, or contralateral; ΔBIC, BIC binocular model - BIC reduced model.

example OMN illustrated in Figs. 1–3 during converging (*A*) versus diverging disconjugate saccades (*B*) in the OFF direction. Notably, when the ipsilateral eye was stationary the firing rate of the neuron stayed relatively constant (*A*). In comparison, when the ipsilateral eye moved more, the neuron's firing rate decreased (*B*). Thus as for ON-directed disconjugate saccades, this neuron, and the majority of the neurons recorded in the study, the neural activity was best predicted when ipsilateral (Fig. 4; superimposed blue trace; $VAF_{pred\text{-}ipsi} = 0.33$), rather than conjugate or contralateral eye positions and velocities (superimposed black and red trace; $VAF_{pred\text{-}conj} = 0.09$ and $VAF_{pred\text{-}contra} = -0.22$), were the model inputs.

As described in detail in the preceding text, we next investigated whether a binocular expansion of the conjugate model would provide an improved description of neuronal discharges during OFF-directed disconjugate saccades. When the parameters of binocular expansion model were freely estimated, a very good description of the example OMN's discharge patterns was obtained (Fig. 4, $VAF_{est\text{-}bino} = 0.51$, *2nd row,* thick black curve). As was true for ON-directed disconjugate saccades, only the ipsilateral eye position (k_i) and ipsilateral velocity sensitivity (r_i) and bias terms were significantly different from zero (Fig. 4*C*). Removing the contralateral eye position (k_c) and contralateral eye velocity-sensitivity term (r_c) had a negligible impact on our ability to fit this neuron's discharge (blue dashed curve, *2nd row,* Fig. 4; $VAF_{est\text{-}ipsi} = 0.50$, $\Delta BIC < 0.01$). We therefore conclude that this neuron is monocular with a preference for the ipsilateral eye.

Summary of ocular preferences

Average predicted and estimated VAFs and differences in BIC provided by the complete binocular versus reduced models during the ON direction are summarized in Table 2. As described previously (Sylvestre and Cullen 2002), a ratio index was used to assign each OMN to one of five ocular categories, namely; monocular ipsilateral, monocular contralateral, binocular ipsilateral, binocular contralateral, or conjugate. Briefly, a ratio of ipsi- and contralateral eye velocity ($Ratio_{vel}$) and a ratio of ipsilateral and contralateral eye position ($Ratio_{pos}$) were computed based on the estimated parameters of the expanded binocular model (see METHODS): Ratio = (smaller estimated parameter value)/(larger estimated parameter value).

Thus for monocular units, where one of the sensitivities was equivalent to zero, the Ratio of the sensitivities is equal to zero. Conjugate units had Ratio value of one since both sensitivities had equal values.

The distributions of $Ratio_{vel}$ and $Ratio_{pos}$ obtained using this method for OMNs is shown in Fig. 5 for ON and OFF directions. With respect to the eye velocity sensitivities, the majority of the neurons (ON: 74%; OFF: 80%) in our sample had monocular velocity sensitivities (i.e., $Ratio_{vel} = 0$; red and blue columns, Fig. 5*A1*). Of the monocular units, the majority of the neurons (ON: 76%; OFF: 89%) encoded the movement of the ipsilateral eye. The distribution of $Ratio_{pos}$ was similar to that of $Ratio_{vel}$ (Fig. 5*B*). The main difference between $Ratio_{vel}$ and $Ratio_{pos}$ was that in the ON direction more neurons (10 vs. 27%) encoded the motion of both eyes with respect to their position sensitivities (i.e., conjugate; Ratio = 1; black columns). For comparison, the distribution obtained for abducens neurons (Sylvestre and Cullen 2002) is shown as an *inset.*

Comparison of ocular preference during disconjugate saccades and disconjugate fixation

We next addressed whether individual OMNs have the same ocular preference during disconjugate saccades and disconjugate fixation. For each neuron, we estimated the mean firing rate during steady periods of disconjugate fixation. We then estimated the mean firing rate as a function of the average ipsilateral and contralateral eye. A $Ratio_{fix}$ value was calculated using the same procedure as described in the preceding text for $Ratio_{pos}$ and $Ratio_{vel}$ (e.g., smaller parameter value/larger parameter value).

Figure 6 illustrates the distribution of $Ratio_{fix}$ during disconjugate fixation. During disconjugate fixation the majority of the neurons (53%) preferred the ipsilateral eye. This distribution is similar to that obtained during disconjugate saccades (compare Figs. 5*A2* and 6). Notably, for the majority of the neurons, the preferred eye estimated during disconjugate fixation was same as the preferred eye estimated during disconjugate saccades. In other words, OMNs have similar ocular preferences during fixation and saccadic behaviors.

Model parameters estimated across oculomotor behaviors: fixation, microsaccades, and saccades

A second goal of this study was to evaluate whether the same linear model relating eye motion to OMN discharge could be applied across different oculomotor behaviors. Velocity and position sensitivities were estimated and compared across three conjugate oculomotor behaviors, namely: fixation, microsaccades, and saccades. Saccades were grouped according to velocity such that faster saccades (>300°/s) could be compared with slower saccades (150–300°/s).

As described previously (Van Gisbergen et al. 1981), we found that OMNs display a small increase in firing rate during miscrosaccades in the neuron's preferred direction. We estimated a neuron's sensitivity to velocity and position during miscrosaccades using the same dynamic model that was shown to accurately describe the neuronal discharge of OMNs during disconjugate and conjugate saccades. This model structure also provided an accurate description of the neuronal discharge during microsaccades (mean population VAF = 0.50 ± 0.18,

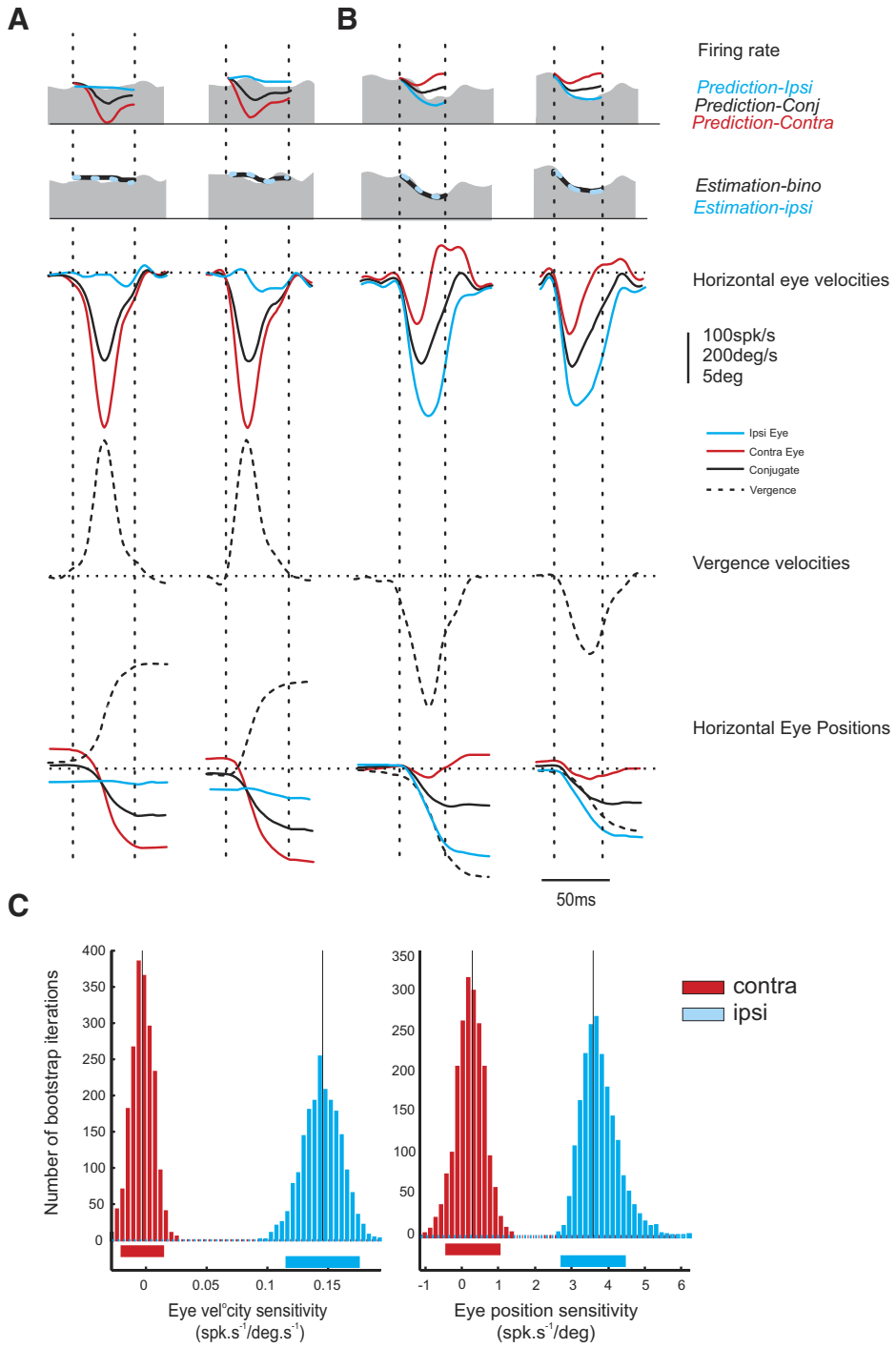

FIG. 4. Discharge patterns of an example monocular neuron during converging (*A*) and diverging (*B*) disconjugate saccades in the neuron's OFF direction. The firing rate of the neuron is shown as the gray shaded area (*top row* and reproduced in *2nd row* for clarity). Predicted model fits using ipsilateral, conjuagte, and contralateral eye velocities are shown in the *top row* in blue, black, and red, respectively (VAF_{ipsi} = 0.33, VAF_{conj} = 0.09, VAF_{contra} = −0.22). Estimated model fits using the binocular model (black trace) and reduced ipsilateral model (dashed blue trace) are shown in the *2nd row*. Note VAFs indicated here were calculated when fitting the entire data set. Conjugate, vergence, and vertical velocities and positions (*bottom rows*) are also shown. Dotted vertical lines represent vertical saccade onsets and offsets. *C*: bootstrap histograms and 95% confidence intervals (thick horizontal bars) for this neuron. Note the 95% confidence interval for the contralateral eye (red bar) overlaps with 0.

bias = 100.6 ± 46.34 spike/s, r = 0.63 ± 0.43(spike/s)/(°/s), k = 6.0 ± 2.9(spike/s)/°).

Coefficient values estimated across the oculomotor behaviors were averaged across neurons and plotted as a function of the mean peak velocity generated during each behavior. Figure 7 highlights the observed trends. Overall, it was found that coefficients values estimated during slower movements differed from faster movements. The eye velocity (r) and eye position (k) coefficients estimated during fast saccades (i.e., >300°/s) were significantly smaller than those estimated during fixation and microsaccades ($P < 0.05$). For comparison, the trends observed for ABN neurons during comparable oculomotor behaviors are also shown (gray dashed trace). We also applied the same model to a data set that included all of the behaviors (e.g., fixation microsaccades, slow saccades, and fast saccades). As expected, the VAF and estimated sensitivities were smaller, albeit not significantly different ($P > 0.05$), from those estimated during the large saccades.

The trends shown in Fig. 7 suggest a nonlinear relationship between eye movement and firing rate. Accordingly, we tested two simple nonlinear models to see whether we could improve our ability to fit neuronal responses. In the first, two higher-order velocity terms were included [e.g., $FR(t) = b + kE(t - t_d) + r_1\dot{E}(t - t_d) + r_2\dot{E}^2(t - t_d) + r^3\dot{E}^3(t - t_d)$]. The addition of

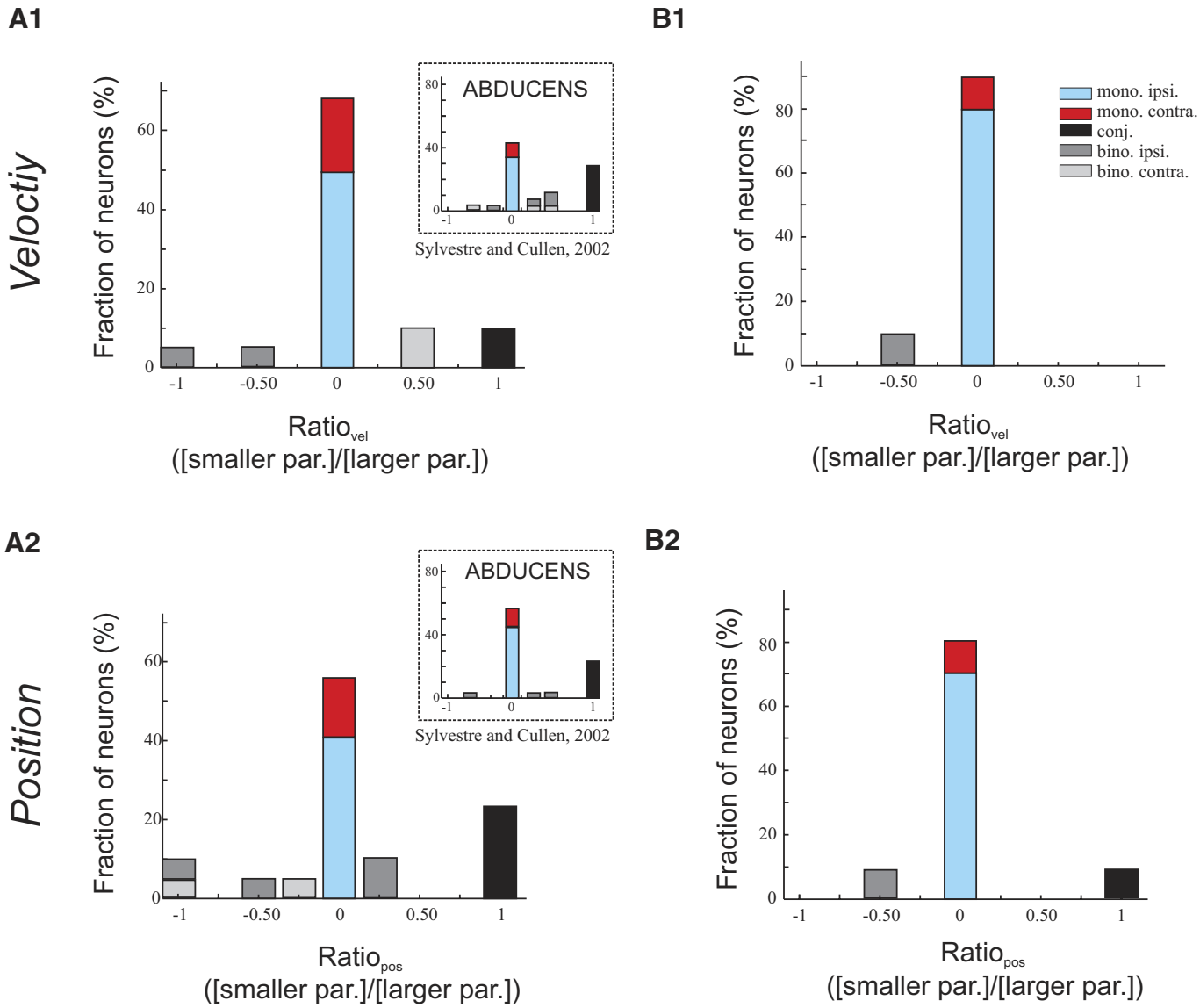

FIG. 5. Distribution of Ratio indexes for oculomotoneurons (OMNs). For each neuron, a Ratio index was calculated for velocity and position sensitivities using: [smaller parameter value]/[larger parameter value], where the smaller and larger parameter values are yielded by the nonpreferred and preferred eyes, respectively in both the ON direction (*A*)and the OFF (*B*) direction. For comparison, the distribution obtained for abducens neurons (Sylvestre and Cullen 2002) is shown as an *inset* in *A*. Similar to abducens motoneuron (ABNs), the majority of the OMNs encoded the velocity and position of the ipsilateral eye (blue bars).

these terms only slightly increased our ability to fit the complete data set (VAF = 0.58 ± 0.09 vs. 0.60 ± 0.09), and the accompanying reduction in the BIC was minimal ($\Delta BIC < 0.05$), suggesting the addition of these terms was not warranted. In the second model, a term to account for an interaction between position and velocity (e.g., $r_2 E \dot{E}$) was included. Again, addition of this term resulted in only a small increase in VAF (0.58 ± 0.09 vs. 0.59 ± 0.09), and minimal change in BIC ($\Delta BIC < 0.05$). Accordingly, we conclude that the nature of the nonlinearity is more complex and most likely reflects the mechanics of the extraocular muscle and/or agonist/antagonist interaction. This point is addressed in the following text and in the discussion.

It has been proposed that the consideration of the activation of the antagonist muscle could account for the increase in sensitivities that is associated with decreasing velocities (Sylvestre and Cullen 1999). For example, during slower movements, the contribution of the antagonist muscle could be providing an additional active force that opposes the agonist muscle. Here we tested this prediction. In particular, we estimated the sensitivities of OMNs during the neuron's OFF direction (i.e., antagonist motoneurons) for the same oculomotor behaviors and compared these responses to those previously published for ABNs (i.e., agonist motoneurons) during comparable oculomotor behaviors (Sylvestre and Cullen 1999). During microsaccades and slow saccades, the neurons did not cease firing, and thus we estimated velocity and position sensitivities during these movements. The estimated sensitivities are shown in Fig. 7 (red trace). During larger movements, the majority of the neurons were driven into inhibitory cut-off, therefore velocity and position sensitivities were not estimated (red asterisks Fig. 7). Taken together, these findings suggest that the antagonist muscle force is not negligible during slower movements and could account for the larger sensitivities re-

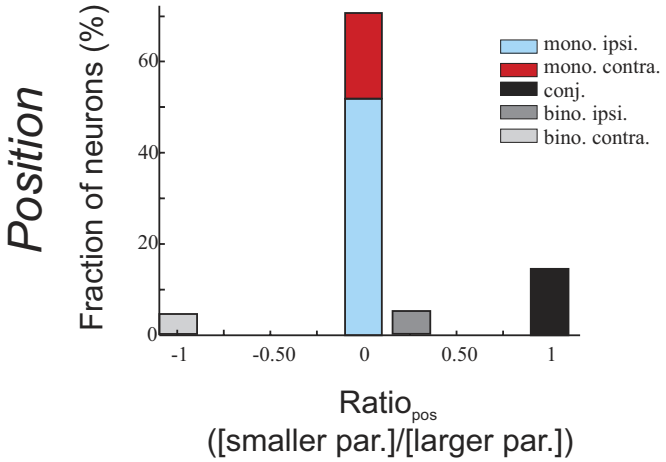

FIG. 6. Distribution of Ratio indexes during disconjugate fixation. A Ratio index was calculated for position sensitivities using: [smaller parameter value]/[larger parameter value], where the smaller and larger parameter values are yielded by the nonpreferred and preferred eyes, respectively.

ported for agonist motoneurons during slow movements. Average sensitivities for each of the oculomotor behaviors, in the ON and OFF direction (i.e., agonist and antagonist, respectively), are summarized in Table 3.

DISCUSSION

In this study, we provide the first detailed characterization of OMNs in the oculomotor nucleus during conjugate and disconjugate saccades. In particular, we determined whether a first-order linear model, which has been previously verified as an accurate description of abducens neurons during conjugate saccades, is also appropriate for describing the neuronal discharge of OMNs. We then determined whether sensitivities estimated during conjugate saccades could be used to accurately predict OMNs discharges during disconjugate saccades. Our main finding was that the discharge dynamics of OMNs are most accurately described using the position and velocity of the ipsilateral eye. Finally, to assess how agonist and antagonist extraocular muscles work together to ensure accurate viewing, the responses of OMNs, across a range of velocities, were compared with the responses of ABNs during comparable oculomotor behaviors.

Dynamic discharge of OMNs during conjugate saccades

Overall, our results clearly demonstrate that a first-order linear model, which includes a bias term, an eye-position term and an eye-velocity term, provides an accurate description of the discharge dynamics of OMNs during ON and OFF directed conjugate saccades. These results are in agreement with prior characterizations of the mechanical properties of the oculomotor plant (Robinson 1964) as well as a detailed characterization of ABNs discharges during conjugate saccades (Sylvestre and Cullen 1999). Notably, including both a slide term and an acceleration term improved the fit by ~10%, similar to the improvement previously described for ABNs (~7%) (Sylvestre and Cullen 1999). Taken together, these findings confirm that first-order linear plant models are a very useful and simple way for describing discharge dynamics of motoneurons during saccades (Robinson 1970; Sylvestre and Cullen 1999, 2002; Van Gisbergen et al. 1981).

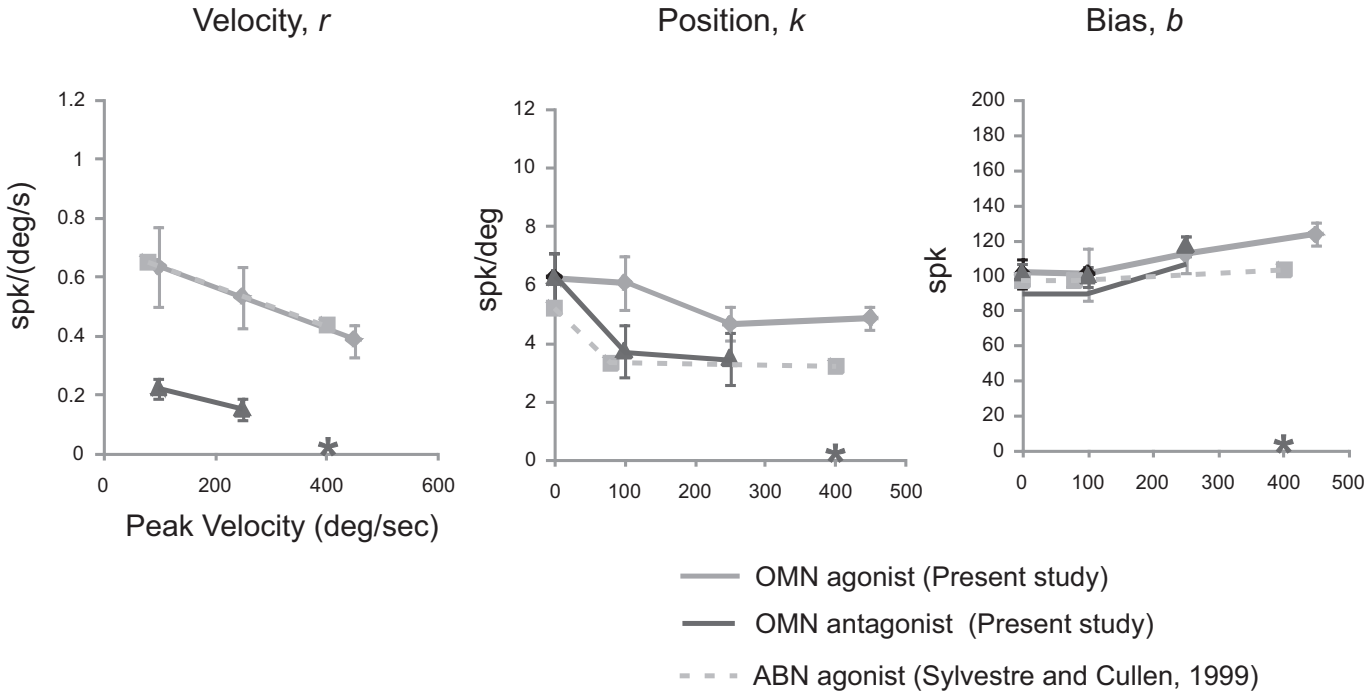

FIG. 7. Eye velocity coefficients (r), eye position coefficients (k), and biases (b) plotted as a function of peak velocity during fixation, microsaccades, slow saccades (150–300°/s) and fast saccades (>300°/s). Data are shown for the subset of neurons for which we had adequate behavior during microsaccades (n = 10). For comparison, the trends observed for ABN neurons during comparable oculomotor behaviors are shown in dashed gray. During larger movements, the majority of the neurons were driven into inhibitory cut-off, therefore velocity and position sensitivities were not estimated (asterisks).

TABLE 3. *Mean model parameters estimated across oculomotor behaviors for agonist and antagonist oculomotoneurons*

Eye Movement	Bias (*b*), spike/s	Position (*k*), (spike/s)	Velocity (*r*), (spike/s)/(°/s)
Fixation	101.1 ± 26.4	6.2 ± 2.67	N/A
Micro saccades (50–150°/s)			
ON	100.6 ± 46.4	6.0 ± 2.9	0.63 ± 0.43
OFF	99.4 ± 27.3	3.7 ± 1.64	0.22 ± 0.14
Small saccades (150–300°/s)			
ON	111.73 ± 33.2	4.6 ± 1.8	0.53 ± 0.32
OFF	117.0 ± 21.3	3.5 ± 1.5	0.07 ± 0.02
Large saccades (>300°/s)			
ON	123.4 ± 20.7	4.8 ± 1.2	0.38 ± 0.17
OFF	N/A	N/A	N/A

Responses of oculomotoneurons during disconjugate fixation and saccades

Previous studies that have evaluated the neural activity of OMNs during vergence have been limited in the respect that they solely evaluated neural activity during static or slow changes in vergence angle (Clendaniel and Mays 1994; Gamlin and Mays 1992; Keller 1973; King et al. 1994; Mays and Porter 1984). It has been shown that OMNs have increased levels of tonic activity with adduction of the ipsilateral eye during both conjugate and convergence movements. OMN discharges were found to be directly proportional to the position of the eye in the orbit. Moreover, this relationship was consistent during both converged and relaxed gaze. In the present study, we confirm that OMN discharges are also directly proportional to the position of the ipsilateral eye in the orbit during disconjugate fixation. Moreover, we provide the first detailed analysis of the discharge dynamics of OMNs during disconjugate saccades. We found that the majority of the neurons (68%) were best described using the movement of the ipsilateral eye. When we investigated whether a binocular expansion of the conjugate model provided an improved description of neuronal discharges during disconjugate saccades, we found that the majority of the neurons were most accurately described using the velocity and position of the ipsilateral eye. Notably, the majority of OMNs had the same ocular preference during disconjugate fixation and saccades.

Comparison of the motor drive of agonist medial and lateral rectus motoneurons during disconjugate saccades

The majority of the neurons in the abducens, which are responsible for driving the lateral rectus muscle, have also been shown to be tuned to the movement of the ipsilateral eye (Sylvestre and Cullen 2002; Zhou and King 1998). A recent neural simulation, of the population drive generated by ABNs during conjugate and disconjugate saccades, revealed that the drive could nearly account for the movement of the ipsilateral eye during disconjugate saccades. However, during disconjugate saccades, the simulated neural activity was 15% smaller than that computed during conjugate saccades (see Fig. 13 Sylvestre and Cullen 2002). In the present study using a similar analysis, we found that the simulated population drive generated during disconjugate saccades was also smaller (~10%) than that generated during conjugate saccades (Fig. 8*A,* ON).

The fact that the neural activity generated during disconjugate saccades is slightly less than that during conjugate saccades is not that surprising if we consider the distribution of ocular preferences of both OMNs and ABNs (see Fig. 5, *inset*). For example, a proportion of both ABNs and OMNs are sensitive to the movement of the contralateral eye. Notably, this finding is also consistent with what is known about the premotor inputs to OMNs and ABNs. While the majority of ABN premotor neurons, such as neurons in the saccade burst generator (Van Horn and Cullen 2008; Van Horn et al. 2008; Zhou and King 1998) and the neural integrator (Sylvestre et al. 2003), are tuned to the movement of the ipsilateral eye, a significant percentage (~40%) are also tuned to the movement of both eyes (i.e., conjugate). Moreover, OMNs receive converging premotor inputs from a number of different neurons that encode vergence angle (e.g., near response neurons) (Judge and Cumming 1986; Zhang et al. 1992) and/or the movement of each eye (e.g., abducens internuclear neurons, and central mesencephalic reticular neurons) (Sylvestre and Cullen 2002; Waitzman et al. 2008).

It is also possible that the difference in neural activity of OMNs and ABNs during conjugate versus disconjugate saccades is offset by the contribution of the antagonist muscle. For example, because the firing rate of OMNs is lower during disconjugate saccades, one might expect the discharge of the antagonist motoneurons (i.e., lateral rectus motoneurons) to also be lower during disconjugate saccades to drive the eye to the same position. However, previous studies, which have evaluated the firing rate of ABNs during disconjugate fixation, suggest that this is not the case. In particular, studies have shown that for a given position of the eye in the orbit, the majority of ABNs actually fire at higher rates during convergence than when gaze is relaxed (Gamlin et al. 1989; Mays and Porter 1984). In the present study, we furthered our understanding of agonist/antagonist interactions by evaluating the dynamic responses of OMNs in the OFF direction (Fig. 8). We found that the population drive generated during disconjugate saccades is the same as that generated during conjugate saccades (Fig. 8*A,* OFF), suggesting a decreased antagonist drive cannot account for differences observed at the level of the abducens when it is the agonist muscle. Taken together, these results suggest that other mechanisms, such as selective weighting, or a sampling bias may be responsible for the apparent missing motoneuron drive during disconjugate saccades (Sylvestre and Cullen 2002).

Indeed there is evidence for the possibility that different motoneurons may contribute more to certain oculomotor behaviors than others. Extraocular muscle, which has two types of muscle fibers: twitch and nontwitch fibers (Buttner-Ennever et al. 2001; Spencer and Porter 1988), receives innervations from different types of motoneurons. Recent retrograde studies have shown that twitch fibers receive innervations from large motoneurons, which lie within the oculomotor nuclei, whereas nontwitch fibers received innervations from small motoneurons, which tend to lie separately around the periphery of the nucleus (Buttner-Ennever 2006; Buttner-Ennever et al. 2001; Ugolini et al. 2006). Moreover, small motoneurons in the abducens have been found to receive innervations from premotor sources involved in executing slow eye movements (e.g., vestibular nucleus, prepositus hypoglossi, and supraoculomotor nucleus), whereas large motoneurons receive premotor signals from the saccadic burst generator (Ugolini et al. 2006; Wasicky et al. 2004) (Fig. 8*B*). In the present study, as well as in previous studies, the neurons recorded were most likely

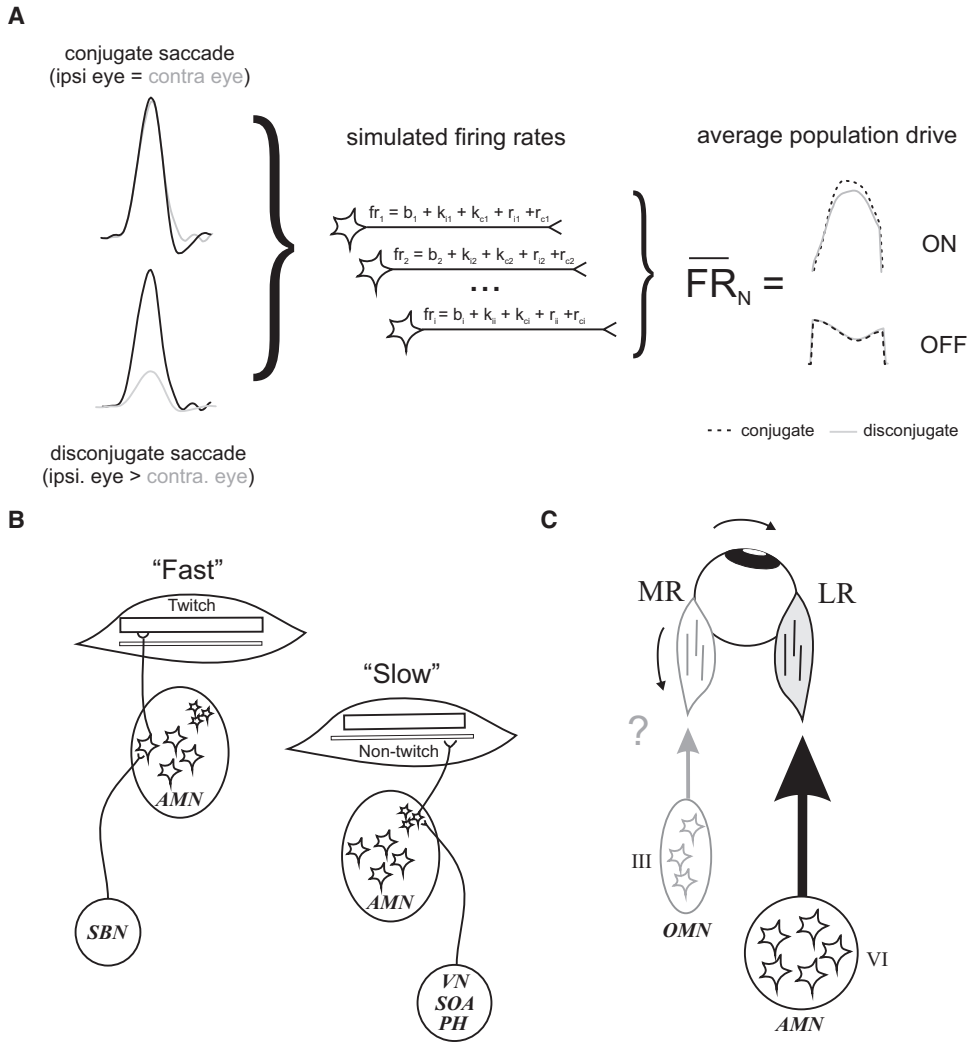

FIG. 8. *A*: a simulation of oculomotor population drive during a conjugate and disconjugate saccade in both the ON and OFF direction. A typical conjugate saccade was selected from the data set. Dynamic models estimated on the actual data were used to reconstruct the firing rate that each neuron in our sample would have generated during this saccade. The resulting *N* firing rates were then averaged to provide an estimate of the population drive (FR_N). A comparable simulation was then performed for a disconjugate saccade that was derived from the example conjugate saccade where the contralateral eye position and velocity was scaled down to 25% of its original amplitude. Notably this was done to ensure that the movement of the ipsilateral eye was identical in the 2 saccades. The average firing rates obtained is shown on the far right for saccades in the ON (*top curves*) and OFF (*bottom curves*) direction. Solid curve is for the conjugate saccade and dotted curve is for the disconjugate saccade. *B*: schematic diagram of muscle fiber innervations. Twitch fibers receive innervations from large motoneurons, which lie within the oculomotor nuclei (*left*), whereas nontwitch fibers received innervations from small motoneurons, which tend to lie separately around the periphery of the nucleus (*right*). Large motoneurons receive premotor signals from the saccadic burst generator (SBN) whereas small motoneurons receive innervations from premotor sources involved in executing slow eye movements [e.g., vestibular nucleus (VN), prepositus hypoglossi (PH) and supraoculomotor nucleus (SOA)]. *C*: schematic diagram of how the contribution of antagonist motoneurons could account for differences in sensitivities observed across oculomotor behaviors.

larger motoneurons within the motor nucleus (e.g., twitch fibers motoneurons). Accordingly, an under sampling of neurons that are more specialized for vergence movements (e.g., nontwitch motoneurons) could account for the observed missing drive during disconjugate saccades.

Consideration of the antagonist muscle when modeling across oculomotor behaviors

Previous studies have shown that a single linear model equation cannot be used to describe the discharge dynamics of motoneurons across different oculomotor behaviors (Fuchs et al. 1988; Gamlin and Mays 1992; Sylvestre and Cullen 1999). For example, an analysis of eye-velocity and -position sensitivities across oculomotor behaviors with different eye velocities have shown they tend to decrease as peak and mean velocity increases (Fuchs et al. 1988; Gamlin and Mays 1992; Sylvestre and Cullen 1999). Here when we compared eye-velocity and -position sensitivities of OMNs during fixation, microsaccades, slow and fast saccades, we also found that both parameters invariably decreased with increasing velocity. These results are consistent with the proposal that the viscosity of the plant is nonlinear (Collins 1971; Collins et al. 1975; Miller and Robins 1992). For example, Collins (1971) showed that the viscosity of the extraocular muscle varied nonlinearly as a function of the muscle's stretch velocity and that the viscosity of passive orbital tissues remains relatively constant across eye velocities. Accordingly, if faster movements have less viscous resistance than slower movements they would require less force and hence velocity and position coefficients would be lower (see DISCUSSION Sylvestre and Cullen 1999).

It has also been proposed that the relative contribution of antagonist motoneurons could account for these differences in sensitivities observed across oculomotor behaviors. For example, during slow movements (e.g., pursuit), the majority of antagonist motoneurons continue to discharge (Sylvestre and Cullen 1999). Thus the contribution of the antagonist muscle is not negligible, but rather it provides an additional active force to oppose that produced by the agonist muscle. Consequently, a given motoneuron might generate the same discharge in two conditions, but depending on the activation of the antagonist muscle, the movement of the eye could differ (Fig. 8*C*). In the present study, we tested the prediction that the antagonist muscle is not necessarily negligible during slower eye movements. We found that during microsaccades and slow saccades in the OFF direction, the motoneurons controlling the antagonist were not completely silent. This finding is consistent with the reports that eye-velocity and -position sensitivities are higher

for slower movements because the agonist muscle has to oppose the contribution of the antagonist muscle.

Taken together, our findings suggest that to model different oculomotor behaviors it is necessary to consider how populations of neurons work together to ensure accurate three-dimensional viewing. Specific behaviors may recruit different populations of neurons as well as different ratios of agonist versus antagonist motoneurons. Accordingly, accounting for the contribution of the antagonist neurons, as well as individual neuronal properties, is essential for fully understanding how particular eye movements are generated.

ACKNOWLEDGMENTS

We thank J. Brooks, M. Jamali, and D. Mitchell for critically reading the manuscript and S. Nuara and W. Kucharski for excellent technical assistance.

GRANTS

This study was supported by the Canadian Institutes of Health Research, the Natural Science and Engineering Research Council of Canada, and the Fonds de la Recherche en Santé du Québec.

REFERENCES

Buttner-Ennever JA. The extraocular motor nuclei: organization and functional neuroanatomy. *Prog Brain Res* 151: 95–125, 2006.

Buttner-Ennever J, Horn A, Scherberger H, D' Ascanio P. Motoneurons of twitch and nontwitch extraocular muscle fibers in the abducens, trochlear, and oculomotor nuclei of monkeys. *J Comp Neurol* 438: 318–335, 2001.

Carpenter J, Bithell J. Bootstrap confidence intervals: when, which, what? A practical guide for medical statisticians. *Statist Med* 19: 1141–1164, 2000.

Carpenter MB, Mc MR, Hanna GR. Disturbances of conjugate horizontal eye movements in the monkey. I. Physiological effects and anatomical degeneration resulting from lesions of the abducens nucleus and nerve. *Arch Neurol* 8: 231–247, 1963.

Clendaniel RA, Mays LE. Characteristics of antidromically identified oculomotor internuclear neurons during vergence and versional eye movements. *J Neurophysiol* 71: 1111–1127, 1994.

Collins C. *The Control of Eye Movements.* New York: American Press, 1971.

Collins CC, O'Meara D, Scott AB. Muscle tension during unrestrained human eye movements. *J Physiol* 245: 351–369, 1975.

Cullen KE, Guitton D. Inhibitory burst neuron activity encodes gaze, not eye, metrics and dynamics during passive head on body rotation. Evidence that vestibular signals supplement visual information in the control of gaze shifts. *Ann N Y Acad Sci* 781: 601–606, 1996.

Cullen KE, Guitton D. Analysis of primate IBN spike trains using system identification techniques. I. Relationship To eye movement dynamics during head-fixed saccades. *J Neurophysiol* 78: 3259–3282, 1997.

Cullen KE, Rey CG, Guitton D, Galiana HL. The use of system identification techniques in the analysis of oculomotor burst neuron spike train dynamics. *J Comput Neurosci* 3: 347–368, 1996.

Fuchs AF, Robinson DA. A method for measuring horizontal and vertical eye movement chronically in the monkey. *J Appl Physiol* 21: 1068–1070, 1966.

Fuchs AF, Scudder CA, Kaneko C. Discharge patterns and recruitment order of identified motoneurons and internuclear neurons in the monkey abducens nucleus. *J Neurophysiol* 60: 1874–1895, 1988.

Gamlin PD, Gnadt JW, Mays LE. Abducens internuclear neurons carry an inappropriate signal for ocular convergence. *J Neurophysiol* 62: 70–81, 1989.

Gamlin PD, Mays LE. Dynamic properties of medial rectus motoneurons during vergence eye movements. *J Neurophysiol* 67: 64–74, 1992.

Hayes A, Richmond BJ, Optican LM. A UNIX-based multiple process system for real-time data acquisition and control. *WESON Conf Proc* 1–10, 1982.

Highstein SM, Baker R. Excitatory termination of abducens internuclear neurons on medial rectus motoneurons: relationship to syndrome of internuclear ophthalmoplegia. *J Neurophysiol* 41: 1647–1661, 1978.

Highstein SM, Karabelas A, Baker R, McCrea RA. Comparison of the morphology of physiologically identified abducens motor and internuclear neurons in the cat: a light microscopic study employing the intracellular injection of horseradish peroxidase. *J Comp Neurol* 208: 369–381, 1982.

Judge SJ, Cumming B. Neurons in monkey midbrain with activity related to vergence eye movement and accomodation. *J Neurophysiol* 55: 915–930, 1986.

Judge SJ, Richmond BJ, Chu FC. Implantation of magnetic search coils for measurement of eye position: an improved method. *Vision Res* 20: 535–538, 1980.

Keller EL. Accomodative vergence in the alert monkey. Motor unit analysis. *Vision Res* 13: 1565–1575, 1973.

King WM, Zhou W, Tomlinson RD, McConville KM, Page WK, Paige GD, Maxwell JS. Eye position signals in the abducens and oculomotor nuclei of monkeys during ocular convergence. *J Vestib Res* 4: 401–408, 1994.

Maciewicz R, Kaneko C, Highstein SM, Baker R. Morphophysiological identification of interneurons in the oculomotor nucleus that project to the abducens nucleus in the cat. *Brain Res* 96: 60–65, 1975.

Mays LE, Porter JD. Neural control of vergence eye movements: activity of abducens and oculomotor neurons. *J Neurophysiol* 52: 743–761, 1984.

Miller JM, Robins D. Extraocular muscle forces in alert monkey. *Vision Res* 32: 1099–1113, 1992.

Robinson DA. The mechanics of human saccadic eye movement. *J Physiol* 174: 245–264, 1964.

Robinson DA. Oculomotor unit behavior in the monkey. *J Neurophysiol* 33: 393–403, 1970.

Robinson DA, Keller EL. The behavior of eye movement motoneurons in the alert monkey. *Bibl Ophthalmol* 82: 7–16, 1972.

Schiller PH. The discharge characteristics of single units in the oculomotor and abducens nuclei of the unanesthetized monkey. *Exp Brain Res* 10: 347–362, 1970.

Spencer RF, Porter JD. Structural organization of the extraocular muscles. *Rev Oculomot Res* 2: 33–79, 1988.

Steiger HJ, Buttner-Ennever J. Relationship between motoneurons and internuclear neurons in the abducens nucleus: a double retrograde tracer study in the cat. *Brain Res* 148: 181–188, 1978.

Sylvestre PA, Choi JT, Cullen KE. Discharge dynamics of oculomotor neural integrator neurons during conjugate and disjunctive saccades and fixation. *J Neurophysiol* 90: 739–754, 2003.

Sylvestre PA, Cullen KE. Quantitative analysis of abducens neuron discharge dynamics during saccadic and slow eye movements. *J Neurophysiol* 82: 2612–2632, 1999.

Sylvestre PA, Cullen KE. Dynamics of abducens nucleus neuron discharges during disjunctive saccades. *J Neurophysiol* 88: 3452–3468, 2002.

Sylvestre PA, Galiana HL, Cullen KE. Conjugate and vergence oscillations during saccades and gaze shifts: implications for integrated control of binocular movement. *J Neurophysiol* 87: 257–272, 2002.

Ugolini G, Klam F, Doldan Dans M, Dubayle D, Brandi AM, Buttner-Ennever J, Graf W. Horizontal eye movement networks in primates as revealed by retrograde transneuronal transfer of rabies virus: differences in monosynaptic input to "slow" and "fast" abducens motoneurons. *J Comp Neurol* 498: 762–785, 2006.

Van Gisbergen JA, Robinson DA, Gielen S. A quantitative analysis of generation of saccadic eye movements by burst neurons. *J Neurophysiol* 45: 417–442, 1981.

Van Horn MR, Cullen KE. Dynamic coding of vertical facilitated vergence by premotor saccadic burst neurons. *J Neurophysiol* 100: 1967–1982, 2008.

Van Horn M, Sylvestre PA, Cullen KE. The brain stem saccadic burst generator encodes gaze in three-dimensial space. *J Neurophysiol* 99: 2602–2616, 2008.

Van Opstal A, Van Gisbergen J, Eggermont J. Reconstruction of neural control signals for saccades based on an inverse method. *Vision Res* 25: 789–801, 1985.

Waitzman DM, Van Horn MR, Cullen KE. Neuronal evidence for individual eye control in the primate cMRF. *Prog Brain Res* 171: 143–150, 2008.

Wasicky R, Horn AK, Buttner-Ennever JA. Twitch and nontwitch motoneuron subgroups in the oculomotor nucleus of monkeys receive different afferent projections. *J Comp Neurol* 479: 117–129, 2004.

Zhang Y, Mays LE, Gamlin PD. Characteristics of near response cells projecting to the oculomotor nucleus. *J Neurophysiol* 67: 944–960, 1992.

Zhou W, King WM. Premotor commands encode monocular eye movements. *Nature* 393: 692–695, 1998.

Zuber B, Semmlow J, Stark L. Frequency characteristics of the saccadic eye movement. *Biophysical J* 8: 1288–1298, 1968.